

Luminescent Benzoquinolate-Isocyanide Platinum(II) Complexes: Effect of Pt...Pt and π ... π Interactions on their Photophysical Properties

Juan Forniés,^{*[a]} Violeta Sicilia,^{*[b]} Pilar Borja,^[a] José M. Casas,^[a] Alvaro Díez,^[c] Elena Lalinde,^[c] Carmen Larraz,^[a] Antonio Martín,^[a] and M. Teresa Moreno^[c]

Abstract: The neutral compounds [Pt(bzq)(CN)(CNR)] (R = *t*Bu (**1**), Xyl (**2**), 2-Np (**3**); bzq = benzoquinolate, Xyl = 2,6-dimethylphenyl, 2-Np = 2-naphthyl) were isolated as the pure isomers with a *trans*-C_{bzq},CNR configuration, as confirmed by ¹³C{¹H} NMR spectroscopy in the isotopically marked [Pt(bzq)(¹³CN)(CNR)] (R = *t*Bu (**1'**), Xyl (**2'**), 2-Np (**3'**)) derivatives ($\delta^{13}\text{C}_{\text{CN}} \approx 110$ ppm; $^1J(\text{Pt},^{13}\text{C}) \approx 1425$ Hz). By contrast, complex [Pt(bzq)(C \equiv CPh)(CNXyl)] (**4**) with a *trans*-N_{bzq},CNR

configuration, has been selectively isolated from [Pt(bzq)Cl(CNXyl)] (*trans*-N_{bzq},CNR) using Sonogashira conditions. X-ray diffraction studies reveal that while **1** adopts a columnar-stacked chain structure with Pt–Pt distances of 3.371(1) Å and significant π ... π interac-

Keywords: coordination chemistry • metallophilic interactions • pi interactions • platinum • stacking interactions

tions (3.262 Å), complex **2** forms dimers supported only by short Pt...Pt (3.370(1) Å) interactions. In complex **4** the packing is directed by weak bzq...Xyl and bzq...C \equiv E (C, N) interactions. In solid state at room temperature, compounds **1** and **2** both show a bright red emission ($\phi = 42.1\%$ **1**, 57.6% **2**). Luminescence properties in the solid state at 77 K and concentration-dependent emission studies in CH₂Cl₂ at 298 K and at 77 K are also reported for **1–4**.

Introduction

It is well known that square-planar Pt^{II} complexes show a remarkable tendency to self-assemble into one-dimensional (1D) architectures directed by Pt^{II}...Pt^{II} interactions.^[1] Typical are the double complex salts (DCS) consisting of infinite alternating stacks of cations and anions with the platinum atoms aligned linearly and separated by approximately 3.3 Å, as the Magnus salt [Pt(NH₃)₄][PtCl₄],^[2] the related [Pt(NH₂R)₄][PtCl₄]^[3] or [Pt(CNR)₄][PtCl₄],^[4] and the well-known DCS [Pt(CNR)₄][Pt(CN)₄].^[4–5] In these cases stacking is largely controlled by electrostatic interactions, but

a small contribution from covalent Pt...Pt bonding interactions is also present.^[6] Such linear-chain structures have been observed not only for complex salts but also for anionic, cationic, or neutral complexes. Illustrative examples are found in the salts of [Pt(CN)₄]²⁻,^[7] [Pt(Ntpty)Cl]²⁺ (Ntpty = 4'-(*p*-nicotinamide-*N*-methylphenyl)-2,2':6',2''-terpyridine),^[8] [Pt(tpy)(C \equiv C–C \equiv CX)]⁺ (tpy = 2,2':6',2''-terpyridine, X = H, C₆H₅, 4-OCH₃-C₆H₄)^[9–10] and [Pt(tpy)Cl]⁺,^[11] and in the neutral complexes [PtCl₂(bpy)] (bpy = bipyridine),^[12] [Pt(CN)₂(bpy)],^[13] [Pt(bpm)Cl₂] (bpm = 2,2'-bipyrimidine),^[14] [Pt(phen)(CN)₂] (phen = phenanthroline),^[14] [Pt(bpy)(NCS)₂],^[14] [*cis*-Pt(CN-*p*-(C₂H₅)C₆H₄)₂(CN)₂],^[15] [*trans*-Pt(CN-*p*-(C₂H₅)C₆H₄)₂(CN)₂],^[16] [Pt(CN*t*Bu)₂(CN)₂]^[17] and [Pt(bzq)Cl(CN*t*Bu)],^[18] (bzq = benzoquinolate; $d_{\text{Pt} \cdots \text{Pt}} = 3.09$ to 3.60 Å). The presence in the complexes of nonbulky π -conjugated systems such as diimine, terpyridyl, or C,N-cyclo-metalated ligands adds π ... π interactions to the Pt^{II}...Pt^{II} interactions as the major forces that determine the supramolecular structures.^[19–20] Significant contribution to the structure's stability is observed when the Pt...Pt distance is less than 3.5 Å^[6] and the separation between aromatic groups^[21] no more than 3.8 Å.

As result of Pt...Pt and/or π ... π interactions, stacked square-planar Pt^{II} complexes very often show intense colors and luminescence due to an emission from a ³MMLCT ³-($d\sigma^*(\text{Pt})_2 \rightarrow \pi^*(\text{L})$) excited state that strongly depends on the extent of such stacking interactions; these photophysical properties are therefore very different from those of the isolated mononuclear complexes.^[22] Ground-state aggregation or oligomerization through Pt^{II}...Pt^{II} and π ... π interactions

[a] J. Forniés, P. Borja, J. M. Casas, C. Larraz, A. Martín
Instituto de Síntesis Química y Catálisis Homogénea (ISQCH)
CSIC—Universidad de Zaragoza
Departamento de Química Inorgánica, Facultad de Ciencias
Pedro Cerbuna 12, 50009 Zaragoza (Spain)
E-mail: juan.fornies@unizar.es

[b] V. Sicilia
Instituto de Síntesis Química y Catálisis Homogénea (ISQCH)
CSIC—Universidad de Zaragoza
Departamento de Química Inorgánica
Escuela de Ingeniería y Arquitectura de Zaragoza
Campus Río Ebro, Edificio Torres Quevedo, 50018, Zaragoza (Spain)

[c] A. Díez, E. Lalinde, M. T. Moreno
Departamento de Química - Grupo de Síntesis Química de La Rioja
UA-CSIC, Universidad de La Rioja
26006, Logroño (Spain)
Fax: (+34)941-299621

Supporting information for this article is available on the WWW under <http://dx.doi.org/10.1002/asia.201200585>.

exist not only in the solid state but also in solution; that is, aggregation of $[\text{Pt}(\text{tpy})(\text{C}\equiv\text{C}-\text{C}\equiv\text{CX})]^+$ ($\text{X}=\text{H}$, C_6H_5 , $4\text{-OCH}_3\text{-C}_6\text{H}_4$) is induced by the variation of solvent composition, causing drastic changes in the absorption and emission colors with no precipitation of the higher nuclearity species.^[9–10,23] Environmental factors such as solvent, vapors, and counterion can perturb the weak $\text{Pt}\cdots\text{Pt}$ and/or $\pi\cdots\pi$ interactions and subsequently modify their associated photophysical properties.^[22,24] In fact, some 1D Pt^{II} compounds have been shown to exhibit vapochromic and vapoluminescent properties, such as the stacked double salts $[\text{Pt}(\text{CNR})_4]$ $[\text{M}(\text{CN})_4]^{25}$ and the neutral complexes $[\text{Pt}^{\text{II}}(\text{CN}-i\text{-C}_3\text{H}_7)_2(\text{CN})_2]^{26}$ and *cis*- $[\text{Pt}(p\text{-CN-C}_6\text{H}_4\text{-C}_2\text{H}_5)_2(\text{CN})_2]^{15}$

In the course of our research we have prepared the chloro isocyanide complexes $[\text{Pt}(\text{bzq})\text{Cl}(\text{CNR})]$ ($\text{R}=\text{tBu}$, Xyl, 2-Np)^[18] and studied their intriguing structural and photophysical properties. As considerable experimental work has demonstrated that the electronic properties of the ligands have a primary effect on the strength of $\text{Pt}\cdots\text{Pt}$ interactions, with stronger field and π -acidic ligands enhancing the interactions,^[1,27–28] we decided to investigate the effect, if any, of the substitution of the chloride by CN^- and $\text{C}\equiv\text{CPh}^-$ in the crystal packing and photophysical properties of the final compounds.

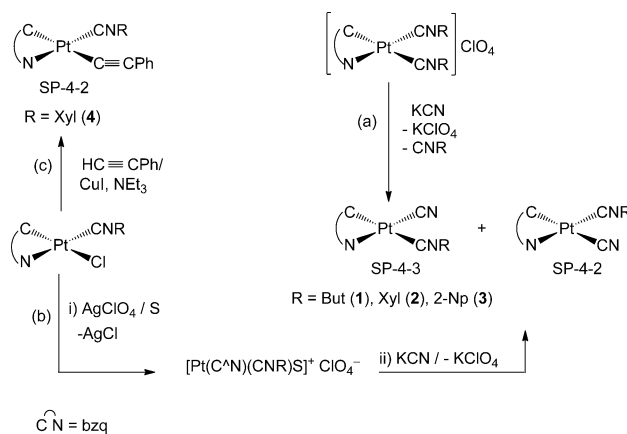
The neutral complexes $[\text{Pt}(\text{bzq})(\text{CN})(\text{CNR})]$ ($\text{R}=\text{tBu}$, Xyl, 2-Np) were first observed in solutions of the double complex salts (DCS) $[\text{Pt}(\text{bzq})(\text{CNR})_2][\text{Pt}(\text{bzq})(\text{CN})_2]$ ($\text{R}=\text{tBu}$, Xyl, 2-Np).^[29] These DCS transform into the corresponding neutral complexes as a mixture of two isomers that could be identified by ^1H and ^{13}C NMR spectroscopy experiments, but no pure samples of any of them could be obtained. For this work, we aimed to prepare pure samples of each isomer of the neutral compounds. The different

strategies followed only allowed us to obtain the (*trans* $\text{C}_{\text{bzq}}\text{-CNR}$) isomer of $[\text{Pt}(\text{bzq})(\text{CN})(\text{CNR})]$ ($\text{R}=\text{tBu}$ (**1**), Xyl (**2**), 2-Np (**3**)) as pure samples. For the purpose of comparison with the isoelectronic complex **2**, compound $[\text{Pt}(\text{bzq})(\text{C}\equiv\text{CPh})(\text{CNXyl})]$ (**4**; *trans*- $\text{N}_{\text{bzq}}\text{-CNR}$) was also prepared, and the photophysical properties of all of them have been also examined.

Results and Discussion

Synthesis and Characterization

With the aim of preparing the neutral compounds $[\text{Pt}(\text{bzq})(\text{CN})(\text{CNR})]$ ($\text{R}=\text{tBu}$, Xyl, 2-Np) as pure single isomers, various strategies were followed. The first consisted of the addition of the equimolar amount of KCN to a solution of $[\text{Pt}(\text{bzq})(\text{CNR})_2]\text{ClO}_4$ ($\text{R}=\text{tBu}$, Xyl, 2-Np) in dichloromethane/methanol (see Scheme 1, path a, and the Experimen-



Scheme 1. Synthetic strategies to **1–4**.

Abstract in Spanish: Los compuestos neutros $[\text{Pt}(\text{bzq})(\text{CN})(\text{CNR})]$ [$\text{R}=\text{tBu}$ **1**, Xyl **2**, 2-Np **3**] fueron aislados como isómeros puros con una configuración *trans*- $\text{C}_{\text{bzq}}\text{-CNR}$, como se confirmó por espectroscopía de RMN de $^{13}\text{C}\{^1\text{H}\}$ de los derivados marcados isotópicamente $[\text{Pt}(\text{bzq})(^{13}\text{CN})(\text{CNR})]$ [$\text{R}=\text{tBu}$ **1'**, Xyl **2'**, 2-Np **3'**] [$\delta^{13}\text{C}_{\text{CN}} \approx 110$ ppm; $^1J(\text{Pt},^{13}\text{C}) \approx 1425$ Hz]. Por el contrario, el complejo $[\text{Pt}(\text{bzq})(\text{C}\equiv\text{CPh})(\text{CNXyl})]$ (**4**) con una configuración *trans*- $\text{N}_{\text{bzq}}\text{-CNR}$, ha sido aislado selectivamente a partir de $[\text{Pt}(\text{bzq})\text{Cl}(\text{CNXyl})]$ (*trans*- $\text{N}_{\text{bzq}}\text{-CNR}$) empleando la reacción de Sonogashira. Los estudios de difracción de rayos X revelan que mientras **1** adopta una estructura de apilamiento en columna con distancias Pt-Pt de 3.371(1) Å e importantes interacciones $\pi\cdots\pi$ (3.262 Å), el complejo **2** forma dímeros unidos solamente por interacciones $\text{Pt}\cdots\text{Pt}$ [3.370(1) Å]. En el complejo **4** el empaquetamiento está dirigido por débiles interacciones $\text{bzq}\cdots\text{Xyl}$ y $\text{bzq}\cdots\text{C}\equiv\text{C}$ (C, N). En estado sólido a temperatura ambiente los compuestos **1** y **2** muestran una emisión roja muy intensa ($\phi=57.6\%$ **2**, 42.1% **1**). Se describen también las propiedades luminiscentes en estado sólido a 77 K y en CH_2Cl_2 en diversas concentraciones a 298 K y a 77 K de **1–4**.

tal Section). These reactions always proceed with replacement of CNR *trans* to N by CN^- to give the neutral complexes (SP-4-3)- $[\text{Pt}(\text{bzq})(\text{CN})(\text{CNR})]$ ($\text{R}=\text{tBu}$ (**1**), Xyl (**2**), 2-Np (**3**)), which were obtained from the reaction mixture as pure samples in very high yields (75–90%). The second strategy consisted of the treatment of $[\text{Pt}(\text{bzq})\text{Cl}(\text{CNR})]$ ($\text{R}=\text{tBu}$, Xyl, 2-Np)^[18] with AgClO_4 (molar ratio 1:1) to abstract the chloride ligand from the coordination sphere of the platinum center as $\text{AgCl}(\text{s})$ and the subsequent addition of KCN (molar ratio 1:1) to the resulting solutions (see Scheme 1, path b, and Experimental Section). Work-up of the reaction mixtures allowed us to obtain the neutral complexes **1–3** as pure samples in moderate yields (48–67%). A third method consisting of the addition of CN^- to a solution of $(\text{NBu}_4)[\text{Pt}(\text{bzq})(\text{CN})_2]$ in dichloromethane was also checked, but substitution of CN^- by CNR was never observed.

Compounds **1–3** were hence obtained in two ways, represented in Scheme 1 (paths a, b) but with very different yields. The moderate yields obtained with the second method (Scheme 1, path b) can be explained because the re-

action always led to mixtures of the two possible isomers SP-4-2 and SP-4-3 (^1H and ^{13}C NMR spectroscopy data are given in the Experimental Section and the Supporting Information), from which only the less soluble one, SP-4-3, could be isolated as a pure substance.

Taking into account that the chloride derivatives $[\text{Pt}(\text{bzq})\text{Cl}(\text{CNR})]$ all reveal a *trans* N, CNR geometry and that the cyanide compounds $[\text{Pt}(\text{bzq})(\text{CN})(\text{CNR})]$ display a *trans* C, CNR geometry, a partial change in the configuration of the Pt center seems to occur. To gain a better insight into this process, the addition of a solution of K^{13}CN in methanol was performed at low temperature (-78°C), and after 1 h the solvent was evaporated to dryness. The ^1H and ^{13}C NMR spectra of these residues showed the presence of both isomers in each case. These mixtures remained unchanged after several days at room temperature in CH_2Cl_2 or after heating them in refluxing acetone. These experimental results indicate that the tetra-coordinated (SP-4-2) and (SP-4-3)- $[\text{Pt}(\text{bzq})(\text{CN})(\text{CNR})]$ compounds, once formed, do not isomerize one into the other, even in refluxing acetone. Therefore, it seems that low-temperature isomerization could take place on the solvent-coordinated species $[\text{Pt}(\text{bzq})(\text{CNR})(\text{S})]^+$ ($\text{S}=\text{acetone}$ or acetonitrile) or, more likely, that the substitution of acetone (OCMe_2) by CN^- proceeds without stereoretention.

The air-stable compounds **1–3** were fully characterized (see the Experimental Section), and for a better characterization, the isotopically marked compounds (SP-4-3)- $[\text{Pt}(\text{bzq})(^{13}\text{CN})(\text{CNR})]$ ($\text{R}=\textit{t}\text{Bu}$ (**1'**), Xyl (**2'**), 2-Np (**3'**)) were synthesized by reaction of $[\text{Pt}(\text{bzq})(\text{CNR})_2]\text{ClO}_4$ ($\text{R}=\textit{t}\text{Bu}$, Xyl, 2-Np) with K^{13}CN according to path a (Scheme 1). All the spectroscopic data indicate that these complexes show a *trans* C_{bzq} , CNR configuration.

Of particular significance are the $^{13}\text{C}\{^1\text{H}\}$ NMR spectra of compounds **1'–3'**, which show a singlet at approximately $\delta=110$ ppm with the corresponding ^{195}Pt satellites, the $^1J(^{195}\text{Pt},^{13}\text{C})$ being about 1425 Hz, as corresponds to a $^{13}\text{CN}^-$ ligand *trans* to N_{bzq} (see Figure 1 for compound **2'**).^[29]

However, treatment of $[\text{Pt}(\text{bzq})\text{Cl}(\text{CNXyl})]$ with excess $\text{HC}\equiv\text{CPh}$ in the presence of the catalytic mixture ($\text{CuI}/$

NEt_3) in chloroform gave rise to the compound (SP-4-2)- $[\text{Pt}(\text{bzq})(\text{C}\equiv\text{CPh})(\text{CNXyl})]$ (**4**, 88% yield) with retention of the *trans*-N,CNR geometry observed in the chloride derivative (see Scheme 1, path c and the Experimental Section). The most informative signals in the $^{13}\text{C}\{^1\text{H}\}$ NMR spectrum of **4** are the expected low-field resonance at $\delta=159.1$ ppm with a large $^1J(^{195}\text{Pt},^{13}\text{C})$ coupling constant (712 Hz), assigned to the metalated carbon atom of the bzq ligand, and the resonances of the C^α and C^β alkyne carbons. The C^α signal appears at $\delta=118.3$ ppm with a platinum coupling constant $^1J(^{195}\text{Pt},^{13}\text{C})$ of 848 Hz, while the C^β alkyne carbon appears shifted to higher field ($\delta=107.8$ ppm), exhibiting a low $^2J(^{195}\text{Pt},^{13}\text{C})=220$ Hz. The relatively low $^{195}\text{Pt}-\text{C}^{\alpha,\beta}$ coupling constants confirm that the alkyne fragment is located *trans* to metalated C_{bzq} atom of high *trans* influence. In fact, these values are in the range of those obtained for alkyne groups located *trans* to the metalated C_{bzq} in $[\text{Pt}(\text{bzq})(\text{C}\equiv\text{CR})_2]$ ($^{195}\text{Pt}-\text{C}^\alpha$ 895–902 Hz, $^{195}\text{Pt}-\text{C}^\beta$ 205–235 Hz).^[30]

X-ray Structures

The X-ray studies on compounds **1** and **2** (Figure 2 and Figure 3) show that they are mononuclear complexes in which the Pt^{II} center is located in distorted square-planar environments formed by the donor atoms of a bzq group, a cyanide ligand, and an isocyanide ligand ($\text{CN}\textit{t}\text{Bu}$ (**1**),

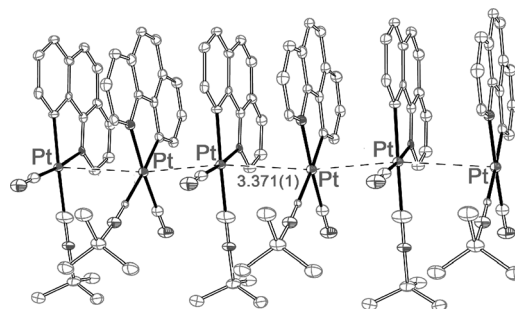


Figure 2. X-ray structure of $[\text{Pt}(\text{bzq})(\text{CN})(\text{CN}\textit{t}\text{Bu})]$ (**1**). Thermal ellipsoids are set at the 50% probability level. H atoms are omitted for clarity.

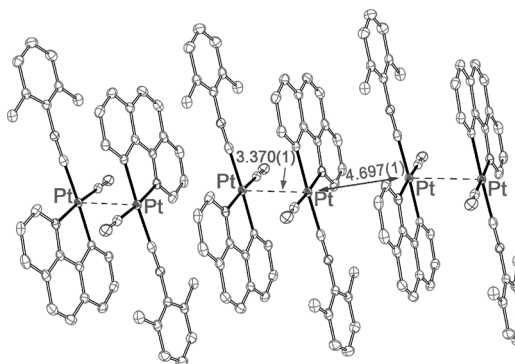


Figure 3. X-ray structure of $[\text{Pt}(\text{bzq})(\text{CN})(\text{CNXyl})]$ (**2**). Thermal ellipsoids are set at the 50% probability level. H atoms are omitted for clarity.

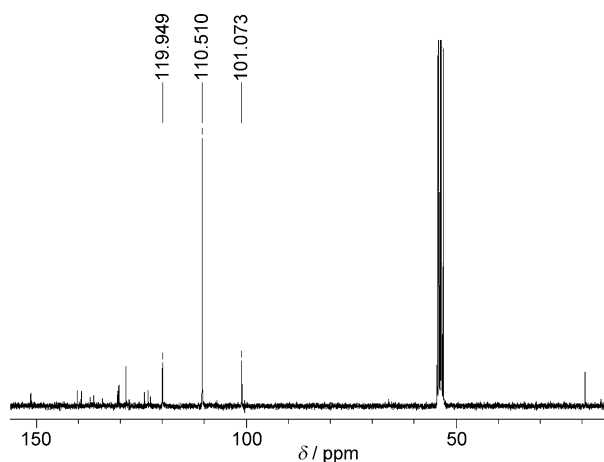


Figure 1. $^{13}\text{C}\{^1\text{H}\}$ NMR spectrum of compound **2'** in CD_2Cl_2 solution.

CNXyl (**2**). In both complexes the CN⁻ is in *trans* position to the N atom of the cyclometalated group. In the case of compound **1**, two molecules with slight differences between each other are present in the crystal. All bond lengths and angles (Table 1) are similar to those observed in platinum complexes containing these kinds of ligands (CN,^[30–31] cyanide^[15,31c,32] and isocyanide^[15–17,31a,33]).

Table 1. Structural data for compounds **1**-CHCl₃ and **2**-CHCl₃.

	Distances [Å] and angles [deg]		
	1 (A)-CHCl ₃	1 (B)-CHCl ₃	2 -CHCl ₃
Pt–C _{CN}	1.933(9)	1.966(8)	1.961(2)
Pt–C _{CNR}	1.989(9)	2.013(7)	1.980(3)
Pt–C _{bzq}	2.024(7)	2.022(7)	2.029(2)
Pt–N _{bzq}	2.060(6)	2.071(6)	2.067(2)
C _{CN} –N _{CN}	1.161(10)	1.140(10)	1.155(3)
C _{CNR} –N _{CNR}	1.142(11)	1.120(9)	1.165(3)
Pt–Pt	3.371(1)	3.371(1)	3.370(1)
C _{CN} –Pt–C _{bzq}	92.7(3)	91.6(3)	92.39(9)
C _{CN} –Pt–C _{CNR}	91.4(3)	94.0(3)	90.67(9)
N _{bzq} –Pt–C _{CNR}	94.3(3)	92.8(3)	95.73(9)
N _{bzq} –Pt–C _{bzq}	81.6(3)	81.6(3)	81.15(8)
Pt–C _{CN} –N _{CN}	178.3(7)	178.0(7)	177.9(2)
Pt–C _{CNR} –N _{CNR}	179.1(7)	178.7(6)	179.5(2)
C–N _{CNR} –C	177.0(8)	173.8(8)	172.6(2)

Both the cyanide and isocyanide ligands are almost linearly coordinated to the platinum center, with bond angles for C and N close to 180°. Complexes **1** and **2** are almost planar; the CN⁻ ligand is in the Pt coordination plane (angles formed by the C–N lines and the normal to plane are 90° **1**, 86.13° **2**) as is the CNR ligand (angles formed by the C–N lines and the normal to plane are 90° **1**, 88.96° **2**).

In complex **2** the Xyl ring is coplanar with the bzq and with the platinum coordination plane; the interplanar angles are 0.69° and 2.10° respectively. The isolated complexes in **1** and **2** are quite similar but differ in the packing arrangement. In complex **1**, the complex units **1**(A) and **1**(B) are arranged in a head-to-head fashion and stacked in a columnar way along the *b* axis through both significant π···π (the shortest atomic separation between two neighboring bzq units is 3.362 Å, below the upper limit of 3.8 Å for this kind of interaction in aromatic compounds^[21]) and metallophilic Pt···Pt interactions (equivalent Pt···Pt–Pt angles of 161.45° and Pt···Pt distances of 3.371(1) Å, shorter than the accepted upper limit of 3.5 Å for these kinds of interactions^[6]). The platinum coordination planes are parallel and lie staggered (torsion angle N–Pt–Pt–C_{bzq} 23.8(2)°), presumably to minimize repulsions and optimize the Pt···Pt and π···π interactions. By contrast, in complex **2**, the molecules are arranged in head-to-tail pairs linked by short Pt···Pt (3.370(1) Å) but not π···π interactions. The dimers are packed in the crystal forming extended 1D chains, but separated by longer distances (Pt···Pt 4.697(1) Å).

The molecular structure of [Pt(bzq)(C≡CPh)(CNXyl)] (**4**, Figure 4, Table 2) confirms that, as in the precursor, the isomer generated has the isocyanide ligand *trans* to the N atom of the bzq group, suggesting that the *trans* influence of

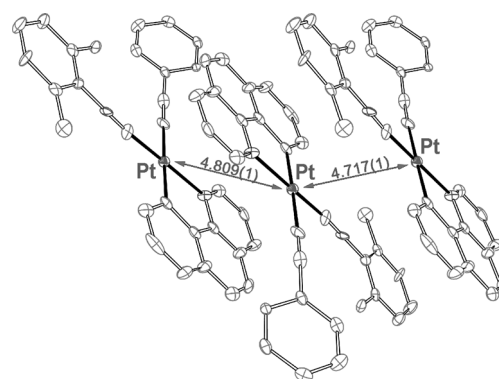


Figure 4. Molecular structure of [Pt(bzq)(C≡CPh)(CNXyl)] (**4**). Thermal ellipsoids are set at the 50% probability level. H atoms are omitted for clarity.

Table 2. Selected structural data for [Pt(bzq)(C≡CPh)(CN-Xyl)] (**4**).

Distances [Å] and angles [deg]			
Pt–C _{C≡Ph}	2.053(13)	Pt–C _{CNR}	1.908(14)
Pt–C _{bzq}	2.051(13)	Pt–N _{bzq}	2.097(10)
C–C _{C≡C}	1.154(19)	C–N _{C≡NR}	1.110(16)
C _{Xyl} –N	1.387(17)		
N _{bzq} –Pt–C _{C≡Ph}	95.1(5)	C ^α –Pt–C ^β _{C≡CPh}	91.0(6)
C _{bzq} –Pt–C _{CNR}	90.3(6)	N _{bzq} –Pt–C _{bzq}	83.5(5)
Pt–C ^α –C ^β _{C≡CPh}	175.4(13)	C ^α –C ^β –C ^γ _{C≡CPh}	176.2(15)
Pt–C–N _{CNR}	175.6(13)	C–N–C _{Xyl}	171.1(14)

the CNXyl ligand is slightly stronger than that of the C≡CPh group. Bond lengths and angles are in the usual ranges for this type of complexes. Both the CNXyl (175.6(13)/171.1(14)°) and C≡CPh (175.4(13)/176.2(15)°) groups show the expected almost linear arrangement. As in **2**, the Xyl ring is coplanar with the Pt coordination plane, but the Ph ring of C≡CPh forms a dihedral angle of 30.52°. The molecules are arranged as head-to-tail pairs by weak π···π interactions (3.60(2) Å) between the bzq ligands and the Xyl rings of the corresponding isocyanides. The dimers form extended 1D chains by weak π···π interactions (ca. 3.5 Å) between the bzq ligands and the C≡E bonds of C≡CPh and CNXyl groups. No metallophilic contacts are observed; the platinum atoms are separated by long distances (Pt···Pt 4.717(1), 4.809(1) Å; Figure 4).

Comparison of the crystal structures of the cyanide compounds **1** and **2** with those of their chloro isocyanide counterparts reveals that **1** shows a 1D crystal packing with significant Pt···Pt (3.371(1) Å) and π···π interactions (3.262 Å), similar to that observed for [Pt(bzq)Cl(CN*t*Bu)·CHCl₃]_∞ (Pt···Pt 3.3547(2) Å). In these cases, neither the electronic effect of the π-acceptor cyanide nor the local geometry around the Pt center significantly affects the crystal structure. However, in [Pt(bzq)(CN)(CNXyl)] (**2**), the molecules are arranged in head-to-tail pairs with short Pt···Pt (3.370(1) Å) but not π···π interactions, while in [Pt(bzq)Cl(CNXyl)], a head-to-tail pairing with one molecule shifted significantly to the side of the other leads to a short (3.293(8) Å) interplanar separation between bzq groups but

no metallophilic interactions. Bearing in mind the nonbulky nature of chloride and cyanide ligands, the metallophilic contacts in **2** could be attributed, to some extent, to the electron-withdrawing character of the cyanide ligand. In complex **4**, in spite of the π -acid character of the acetylide ligand, the expected metallophilic interactions were not observed, but rather $\pi\cdots\pi$ interactions between bzq and Xyl rings and the bzq group and the C–C and C–N triple bonds of $C\equiv CPh$ and $C\equiv NXyl$ groups. Therefore, complex **4** is another example in which the supramolecular structure seems to be determined by a delicate balance of the overall noncovalent intermolecular interactions.

Photophysical Properties

Absorption Spectra

Complexes **1–3** show low solubility in common organic solvents. The electronic absorption spectra of **1–4** were recorded in CH_2Cl_2 at low concentration (5×10^{-5} M, Figure 5) and

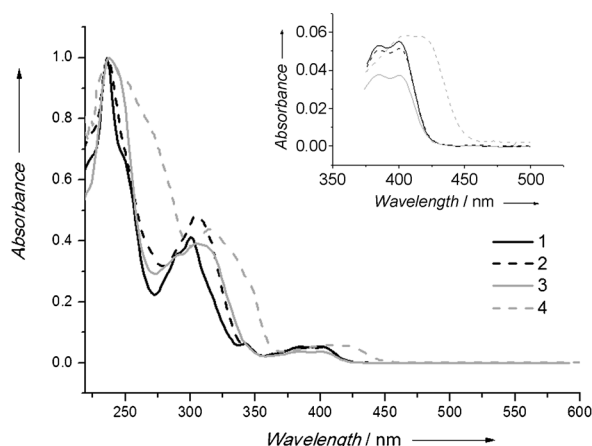


Figure 5. UV/Vis spectra of **1–4** in CH_2Cl_2 (5×10^{-5} M) at 298 K. The inset shows the low-energy region.

the data are summarized in Table 3. As can be seen in Figure 5 they reveal several intense absorptions at λ_{max} values ranging from 225 to 325 nm ($\epsilon > 10^4$ M $^{-1}$ cm $^{-1}$), which can be considered to be mainly due to intraligand (IL, bzq, CNR) and metal-perturbed ligand transitions, most likely with contributions from 1MLCT and $^1LL'CT$ transitions (L = bzq, L' = CNR), as determined by DFT calculations in the analogous compounds [Pt(bzq)Cl(CNR)].^[18]

The less intense low-energy (LE) absorptions, which are slightly blue-shifted ($\lambda > 325$ –400 nm) in relation to the precursors [Pt(bzq)Cl(CNR)]^[18] (CH_2Cl_2 , R = *t*Bu 410, Xyl 412, 2-Np 414 nm), are ascribed to a mixture of spin-allowed metal-to-ligand charge transfer 1MLCT ($d\pi(Pt) \rightarrow \pi^*(bzq)$) and 1ILCT ($bzq, \pi \rightarrow \pi^*$) transitions. This assignment is in line with previous work^[18,31a,34] and with the observed hypsochromic shift due to the substitution of chloride by the acidic cyanide group. Contributions of $^1LL'CT$ or metal-to-

isocyanide charge transfer 1MLCT ($d\pi(Pt) \rightarrow \pi^*(CNR)$) transitions to the LE absorptions bands, if any, must be very low in complexes **1–3**, since these bands show no dependence on the isocyanide substituent (see inset in Figure 5).

By contrast, the lowest energy absorption band in the alkynyl complex **4** is remarkably red-shifted with respect to the related cyanide derivative **2** (423 nm **4** vs. 400 nm **2**). By analogy with other alkynyl cycloplatinate compounds,^[30,35] this band can be assigned to a mixed 1MLCT and alkynyl to bzq ($L'CT$) transition. The observed bathochromic shift of this band in complex **4** in relation to **2** and the chloride precursor (412 nm) is consistent with the expected destabilization of the cyanide or chloride group by the more electron-rich alkynyl ligand. In all complexes, the lowest energy absorption band obeys Beer's law in the range from 5×10^{-5} M to 10^{-3} M (complexes **1, 2, 4**) or from 5×10^{-4} M to 10^{-5} M (complex **3**), which suggests no ground-state aggregation within these concentration ranges.

The solid diffuse reflectance UV/Vis spectrum of **4** shows no differences with respect to that observed in CH_2Cl_2 (Figure 6, Table 3), in accord with the lack of Pt \cdots Pt or

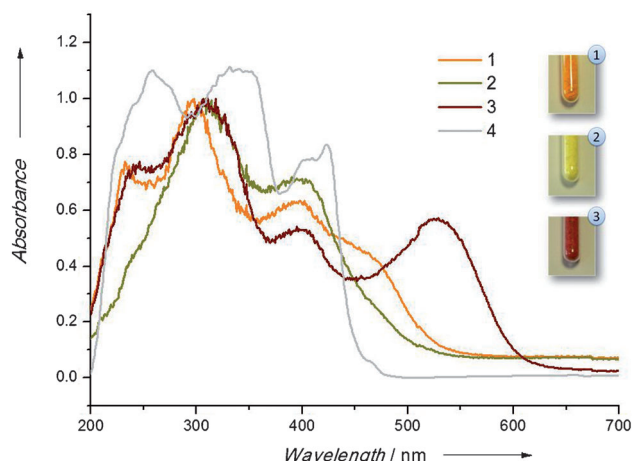


Figure 6. Normalized absorption spectra calculated from the reflectance diffuse spectra of **1–4** in the solid state at 298 K. The photographs show compounds **1–3** in the solid state.

bzq \cdots bzq interactions. Something similar was observed for the yellow compound **2**, which showed no effect of the short Pt \cdots Pt (3.3703(2) Å) distances in the dimers. By contrast, the 1D extended orange compound **1** and the fuchsia compound **3** show absorption bands centered at approximately 460 and 530 nm, respectively. This LE absorption band is responsible for their colors and may be ascribed to 1MMLCT ($d\sigma^*(Pt) \rightarrow \sigma(\pi^*,CN)$) transition with somewhat of an “excimeric” ($\sigma^*(\pi, bzq) \rightarrow \sigma(\pi^*, bzq)$)^[9,18,19b,22,24a,34,36] character, as in other square-planar platinum(II) complexes containing Pt \cdots Pt and $\pi\cdots\pi$ interactions.

Table 3. Absorption and emission data for compounds 1–4.

Compound	$\lambda_{\text{absorption}}$ [nm] ($10^3 \epsilon$ [$\text{M}^{-1} \text{cm}^{-1}$])	$\lambda_{\text{em}} (\lambda_{\text{exc}})$ [nm] [ϕ [%]]	τ [μs]	
1	solid, 298 K	232, 298, 398, 460 sh tail to 540	639 (400–450) [42.1] (639)	0.4 (58%), 1.4 (42%) (639)
	solid, 77 K		660 (450) (660); 720 (550)	0.1 (24%), 2.3 (76%) (660); 1.8 (720)
	CH_2Cl_2 10^{-3} M, 298 K		576 max, 670 sh (400)	0.5 (576)
	CH_2Cl_2 5×10^{-5} M, 298 K ^[a]	236 (51.2), 290 sh (18.3), 300 (21.0), 342 (3.2), 386 (2.7), 400 (2.8)	484, 500, 518, 566 (400)	
	CH_2Cl_2 10^{-3} M, 77 K		535, 594, 653, 718 max (400)	1.2 (730)
2	solid, 298 K	308, 405 tail to 500	482, 512, 662 max (400) [57.6] (662)	25.4 (482); 20.8 (89%), 97.3 (11%) (512); 2.4 (662)
	solid, 77 K		500, 509, 549 max, 582 sh, 680 sh (400)	80.1 (31%), 265.4 (69%) (500); 120.5 (64%), 310.6 (36%) (509); 13.7 (75%), 213.9 (25%) (549); 0.7 (715)
	CH_2Cl_2 10^{-3} M, 298 K		475 sh, 583, 645 sh, 690 max (400)	0.4 (475); 0.4 (575); 1.5 (645); 1.2 (690)
	CH_2Cl_2 5×10^{-5} M, 298 K ^[a]	236 (47.9), 304 (23.2), 386 (2.4), 400 (2.4)	482, 510 sh, 575 max (400)	
	CH_2Cl_2 10^{-3} M, 77 K		650 sh, 750 max (400–475) (750 (520))	2.9 (650) (3.6 (750))
3	solid, 298 K	246, 306, 395, 530 tail to 600	679 (400–550)	0.1
	solid, 77 K		745 (400–550)	1.3
	CH_2Cl_2 5×10^{-5} M, 298 K ^[a]	238 (82.2), 290 sh (29.0), 304 (32.1), 384 (3.1), 400 (3.1)	570, 698 (400)	
	CH_2Cl_2 5×10^{-4} M, 77 K		752 (500) (778 (550))	
4	solid, 298 K	257, 347, 426, 466 sh	480, 505, 517, 580 max (400) [13.3]	12.1 (505); 9.8 (13%), 3.0 (87%) (580)
	solid, 77 K		500 max, 513, 542, 587 sh (400)	193 (500)
	CH_2Cl_2 5×10^{-5} M, 298 K ^[a]	237(58.6), 315(26), 333(21.1), 348(14.8), 400(3.3), 423(3.7)	490 max, 550 (400)	
	CH_2Cl_2 10^{-3} M, 77 K		490, 525, 570 max (400)	
	CH_2Cl_2 5×10^{-5} M, 77 K		490 max, 525, 570 (400)	

[a] The emission pattern was identical to that observed at a concentration of 5×10^{-4} M.

Emission Spectra

Complexes 1–4 are photoluminescent both at room and low temperature (77 K) in the solid state and in CH_2Cl_2 solution (Table 3). In the solid state at 298 K, powdered samples of 1–3 show broad structureless bands with maxima at 639 (1), 662 (2), and 679 nm (3; Figure 7 and Figure 8 and Figures S1

and S2 in the Supporting Information) that, only for 2, appears together with two weak bands at 482 and 512 nm when $\lambda_{\text{exc}} = 400$ nm. The emission efficiency follows the trend $2 > 1 > 3$ ($\phi = 57.6\%$ (2), 42.1% (1); inset in Figure S1 in the Supporting Information). Upon cooling at 77 K, 1 and 2 exhibit site-selective emission. Thus, the emission band in 1 at 298 K splits into two structureless symmetric bands at 660 nm and 720 nm, which can be selectively obtained upon excitation at 450 and 550 nm, respectively (Figure 7).

The excitation spectra monitored at the two emission maxima differ by 0.22 eV, which suggest that each emission band corresponds to a different emissive state. The presence of two close emissive states is a common phenomenon in platinum(II) complexes containing π -extended ligands, which undergo $\pi \cdots \pi$ and/or Pt \cdots Pt stacking. In view of the observed Pt \cdots Pt and $\pi \cdots \pi$ contacts in its crystal structure and recent calculations, these emissions are assigned to mixed $^3\pi\pi^*/^3\text{MMLCT}$ transitions, the low-energy one having a predominant $^3\text{MMLCT}^3$ -($d\sigma^*(\text{M})_2 \rightarrow \pi^*(\text{bzq})$) character and probably some $^3\text{MMCT}^3$ -($d\sigma^* \rightarrow p(\sigma)$) contribution, as in other stacked platinum chain systems.^[17–18,37] In compound 2, the emission spectra at 77 K (Figure 8) change dramatically with the excitation wavelength: a green emission ($\lambda_{\text{max}} = 549$ nm, additional bands at 500, 509, 680(sh) nm) or a red one ($\lambda_{\text{max}} = 715$ nm) are obtained upon excitation at $\lambda_{\text{exc}} = 400$ or 500 nm, respectively.

As expected, the excitation spectra for these two emissions are quite different; the green emission can be attributed to excited states of the monomer species, mostly ^3LC and $^3\text{MLCT}$, while the red-shifted band (715 nm) can be assigned to $^3\text{MMLCT}$ excited states in emissive aggregates. The weak band of 3 becomes narrower and shifts to the red (745 nm)

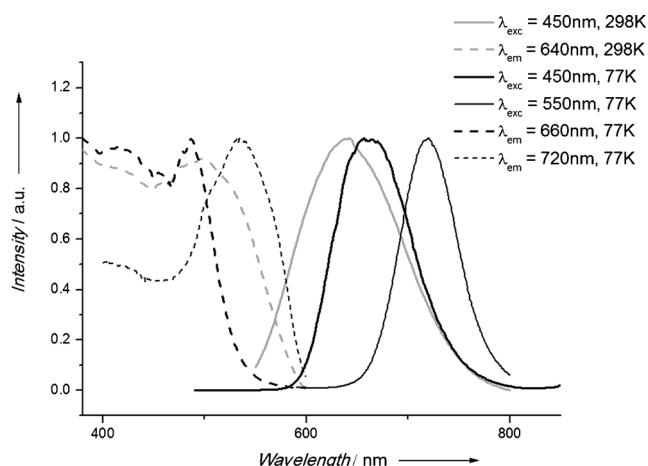


Figure 7. Normalized excitation and emission spectra of **1** in the solid state at 298 and 77 K.

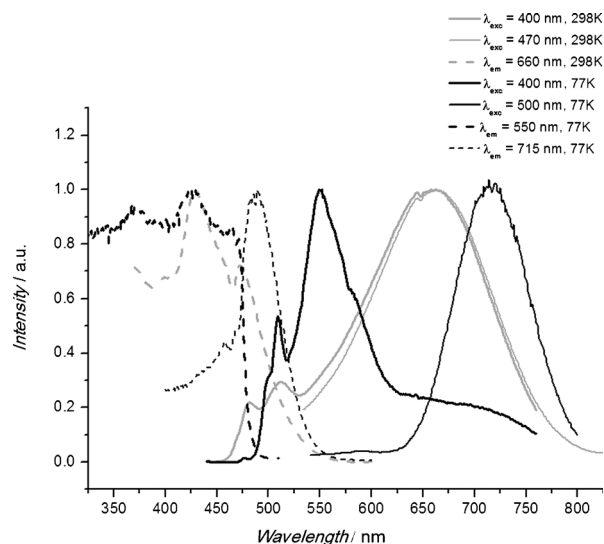


Figure 8. Normalized excitation and emission spectra of **2** in the solid state at 298 and 77 K.

at 77 K (Figure S2 in the Supporting Information), as expected for an emission due to $^3\text{MMLCT}/^3\pi\pi^*$ transitions with predominant $^3\text{MMLCT}$ contribution, associated with aggregates with relatively strong Pt...Pt and $\pi\cdots\pi$ interactions.^[18,22–23,36b–d,37a]

A concentrated solution of **1** (10^{-3}M) in CH_2Cl_2 at 298 K displays a broad band from 450 to 750 nm with its maximum at 576 nm (Figure 9). The excitation spectra monitored at different frequencies resemble its absorption spectrum, indicating that the emission is mainly due to monomer species and excimers formed by interaction ($\pi\cdots\pi$ and/or Pt...Pt) of an excited molecule with an adjacent ground-state one. Solutions of **2** (10^{-3}M) and **3** ($5\times 10^{-4}\text{M}$) in CH_2Cl_2 show analogous behavior, but in these complexes a more important contribution associated with excimers of relatively low energy is clearly observed.

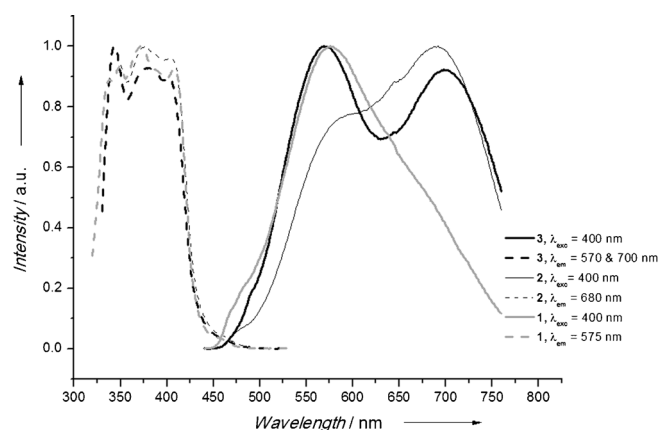


Figure 9. Normalized excitation and emission spectra of **1** (10^{-3}M), **2** (10^{-3}M), and **3** ($5\times 10^{-4}\text{M}$) at 298 K in CH_2Cl_2 .

For compounds **1** and **2** the intensity of the emission band decreases as the concentration decreases from 10^{-3}M to $5\times 10^{-4}\text{M}$, and the band shape also changes (see Figures S3 and S4 in the Supporting Information for **1** and **2** respectively), with the excimeric emission becoming less important as the concentration decreases. For compound **3**, study of the emission at different concentrations is precluded due to its scarce solubility.

The emission profiles of **1–3** change dramatically in rigid matrix of CH_2Cl_2 (77 K, Figure 10). In all cases an intense low-energy $^3\text{MMLCT}$ emission ($\lambda = 730$ (**1**), 750 (**2**), 778 nm

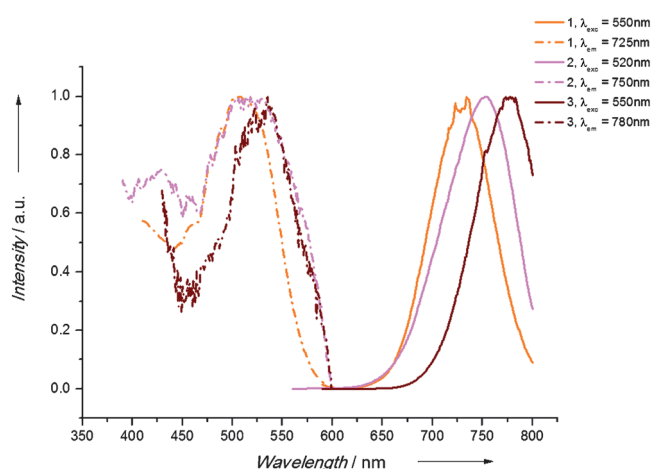


Figure 10. Normalized excitation and emission spectra of **1** (10^{-3}M), **2** (10^{-3}M), and **3** ($5\times 10^{-4}\text{M}$) at 77 K in rigid matrix of CH_2Cl_2 .

(**3**) can be obtained upon excitation at $\lambda = 550$ (**1**), 520 (**2**), 550 nm (**3**). The corresponding excitation spectra monitored in these maxima indicate that these emissions are mainly due to ground-state aggregates formed through Pt...Pt and/or $\pi\cdots\pi$ stacking interactions.

For complexes **1** and **3**, both the emission and the excitation spectra in rigid matrix of CH_2Cl_2 (77 K) resemble those observed in the solid state at 77 K. However, for complex **2** the green emission (ca. 500–600 nm) observed in the solid

state upon excitation at 400 nm was not observed in rigid matrix of CH_2Cl_2 , and the LE band is notably red-shifted (750 nm, glassy CH_2Cl_2 vs. 715 nm, solid 77 K). This feature may be associated with the formation of aggregates with a closer proximity in the glass than in the solid state.

Powdered samples of the alkynyl isocyanide complex **4** exhibit a high-energy (HE) structured band (480, 505, 517 nm) at 298 K, which is ascribed to a typical mixed ${}^3\text{LC}/{}^3\text{MLCT}$ transition of the monomer species, together with LE emission of ${}^3\pi\pi^*$ excimeric nature with its maximum at 580 nm (Figure 11). In keeping with this notion, the excitation spectra monitored at 505 and at 580 nm are essentially coincident. The quantum yield (13.3%) is considerably lower than in **1** and **2**.

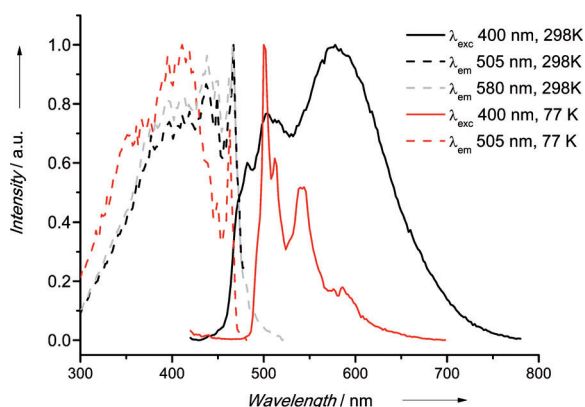


Figure 11. Normalized excitation and emission spectra of **4** in the solid state at 298 K and 77 K.

Lifetime measurement in the maximum (580 nm) fit to two components ($\tau = 9.8 \mu\text{s}$ (13%), $3.0 \mu\text{s}$ (87%)), the long component (dominant in the high-energy peaks 12.1 μs (505 nm)) is attributed mainly to the structured ${}^3\text{LC}$ emission, whereas the short component is attributed to excimeric ${}^3\pi\pi^*$ emission. Upon cooling to 77 K, the LE band almost disappears, and only the structured HE emission, with $\lambda_{\text{max}} = 500 \text{ nm}$, is observed (Figure 11). The long lifetime (193 μs), which fits well to monoexponential decay, is indicative of emission with primarily ${}^3\text{LC}$ parentage. Both in diluted ($5 \times 10^{-5} \text{ M}$) and concentrated (10^{-3} M) deaerated CH_2Cl_2 solutions at room temperature, this complex only exhibits the structured emission profile of the monomer ($\lambda_{\text{max}} 490 \text{ nm}$). At 77 K an additional excimeric feature located at 570 nm is also observed, the intensity of which clearly increases with concentration (Figures S5 and S6 in the Supporting Information).

The bright luminescence of **1** and **2** at 298 K in the solid state at 298 K contrasts with the weak or nonluminescence of the related chloro isocyanide compounds. This fact can be related to the stronger-field nature of the cyanide compared to chloride, which increases the energy gap ΔE between the lowest-lying excited state and the higher-lying nonradiative d-d state. In addition, the electron-withdrawing character of

the cyanide seems to strengthen the Pt...Pt interactions in such a way that the phosphorescent emission of compounds **1–3** in rigid media (solid or rigid matrix in CH_2Cl_2) has a predominant ${}^3\text{MMLCT } {}^3(d\sigma^*(\text{M})_2 \rightarrow \pi^*(\text{bzq}))$ character. However, in complex **4**, in spite of the π -acid character of the alkynyl ligand, no metallophilic interactions are present, and therefore, its luminescence behavior resembles that of the related chloro derivative $[\text{Pt}(\text{bzq})\text{Cl}(\text{CNXyl})]$.^[18]

Conclusions

Compounds $[\text{Pt}(\text{bzq})(\text{CN})(\text{CNR})]$ ($\text{R} = t\text{Bu}$ (**1**), Xyl (**2**), 2-Np (**3**)) and $[\text{Pt}(\text{bzq})(\text{C}\equiv\text{CPh})(\text{CNXyl})]$ (**4**) have been obtained from the corresponding chloro isocyanide derivatives $[\text{Pt}(\text{bzq})\text{Cl}(\text{CNR})]$. The isolated cyanide compounds show a $\text{trans-C}_{\text{bzq}}\text{CNR}$ configuration in contrast to a $\text{trans-N}_{\text{bzq}}\text{CNR}$ observed for complex **4** and the starting chloro compounds. A more efficient and selective way to obtain **1–3** is by reaction of $[\text{Pt}(\text{bzq})(\text{CNR})_2]\text{ClO}_4$ ($\text{R} = t\text{Bu}$, Xyl, 2-Np) with equimolar amount of KCN.

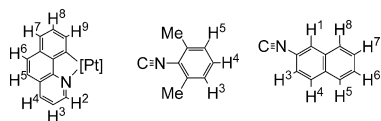
X-ray studies on single crystals reveal that **1** shows a columnar-stacked chain structure with significant Pt...Pt (3.371(1) Å) and $\pi\cdots\pi$ (3.262 Å) interactions. These interactions are similar to those observed for the precursor $[\text{Pt}(\text{bzq})\text{Cl}(\text{CN}t\text{Bu})\cdot\text{CHCl}_3]_{\infty}$, suggesting that in this case neither the electronic effect of the π -acceptor cyanide ligand nor the local geometry around the Pt center have a significant effect on the crystal structure. However, in $[\text{Pt}(\text{bzq})(\text{CN})(\text{CNXyl})]$ (**2**), the molecules are arranged in head-to-tail pairs with short Pt...Pt (3.370 (1) Å) interactions, contrasting with the precursor $[\text{Pt}(\text{bzq})\text{Cl}(\text{CNXyl})]$, which displayed $\pi\cdots\pi$ (3.293(8) Å, $\text{bzq}\cdots\text{bzq}$) interactions, but not metallophilic interactions. In this case the metallophilic contacts in **2** could be attributed to the electron-withdrawing character of the cyanide ligand. However, in spite of the presence of the π -acidic acetylide ligand, no metallophilic interactions were observed in related complex **4**, and its solid structure is mainly determined by a subtle balance of different ($\text{bzq}\cdots\text{Xyl}/\text{C}\equiv\text{C}/\text{C}\equiv\text{N}$) interactions between molecules.

Pt...Pt and/or $\pi\cdots\pi$ contacts present in the cyanide derivatives (**1–3**) affect their emission properties in rigid media showing, in the solid state and in glasses, characteristic ${}^3\text{MMLCT}$ and/or ${}^3\pi\pi^*$ excimeric low-energy features. However, in liquid CH_2Cl_2 the emissions are due to monomer and excimer species, with the excimeric emission becoming more important as the concentration increases. In agreement with the crystal packing, the alkynyl isocyanide complex **4** does not show low-energy ${}^3\text{MMLCT}$ features. This complex displays a typical emission of the monomer species and it is only at 298 K in solid state or in rigid matrix of CH_2Cl_2 at 77 K that an additional low-energy emission of ${}^3\pi\pi^*$ excimeric nature is also observed.

Experimental Section

General Procedures and Materials

The starting materials [Pt(bzq)(CNR)₂]ClO₄^[31a] and [Pt(bzq)Cl(CNR)]^[18] (R = *tert*-butyl, 2,6-dimethylphenyl, 2-naphtyl) were prepared as described elsewhere. K¹³CN and KCN were used as purchased from Isotec. Elemental analyses were carried out with a EuroEa or CE Instrument EA1110 elemental analyzers. IR spectra were recorded on a Perkin-Elmer Spectrum 100 or on a Nicolet Nexus FTIR spectrometer (ATR in the range 250–4000 cm⁻¹). Mass spectra analyses were performed with a Microflex MALDI-TOF Bruker or an Autoflex III MALDI-TOF Bruker instrument. NMR spectra were recorded on a Varian Unity-300 and a Bruker AV-400 spectrometer using the standard reference SiMe₄ (TMS) for ¹H and ¹³C. All of the ¹³C spectra were proton-decoupled, *J* is given in Hz, and assignments are based on ¹H–¹H COSY experiments. The NMR spectral assignments follow the numbering in Scheme 2.



Scheme 2. Numbering for NMR spectral assignment.

Diffuse reflectance UV/Vis (DRUV) spectra were recorded on a Thermo Electron Corporation Evolution 600 or on a Shimadzu UV-3600 spectrophotometers equipped with a Praying Mantis integrating sphere. The solid samples were homogeneously diluted with silica. The absorption spectra were obtained using the Kubelka–Munk transformation of the reflectance spectra. Steady-state photoluminescence spectra were recorded on a Jobin–Yvon Horiba Fluorolog FL-3-11 Tau 3 spectrofluorimeter using band pathways of 3 nm for both excitation and emission. Phosphorescence lifetimes were recorded with a Fluoromax phosphorimeter accessory containing a UV xenon flash tube with a flash rate between 0.05 and 25 Hz. Phase shift and modulation were recorded over the frequency range of 0.1–100 MHz. Nanosecond lifetimes were recorded with an IBH 5000F coaxial nanosecond flashlamp. Quantum yields in the solid state were measured upon excitation at 400 nm (**2**, **4**), 450 nm (**1**), using an F-3018 Integrating Sphere mounted on a Fluorolog FL-3-11-Tau3 spectrofluorimeter. Data were fitted using the Jobin–Yvon software package and the Origin 7.5 program.

Synthesis of (SP-4-3)-[Pt(bzq)(CN)(CN-*t*Bu)] (**1**)

Method a) KCN (0.015 g, 0.23 mmol) and MeOH (30 mL) were added to a solution of [Pt(bzq)(CN-*t*Bu)]ClO₄ (0.148 g, 0.23 mmol) in CH₂Cl₂ (9 mL) and the mixture was stirred for 40 min. The bright yellow solution was then evaporated to dryness and CH₂Cl₂ (65 mL) was added to the residue. Subsequently, the mixture was filtered, the solution was evaporated to dryness, and the orange solid **1** was filtered and washed with Et₂O (5 mL). Yield: 0.080 g, 75%. **Method b)** AgClO₄ (0.062 g, 0.30 mmol) was added to a solution of [Pt(bzq)Cl(CN-*t*Bu)] (0.148 g, 0.30 mmol) in dichloromethane/acetone (25/2 mL) at 0 °C and the mixture was stirred for one hour. It was then filtered through Celite, and KCN (0.020 g, 0.30 mmol), MeOH (2 mL) and H₂O (3 mL) were added to the resulting solution. The mixture was stirred for 1 hour at 0 °C and 1 hour at room temperature. Subsequently, MgSO₄ was added and the mixture was stirred for a while and then filtered through Celite. The solution was evaporated to dryness and the orange residue was treated with CH₂Cl₂ (5 mL). The red solid, **1**, was filtered and dried. Yield: 0.077 g, 48%. ¹H NMR (400.13 MHz, [D₆]acetone, 25 °C, TMS): δ = 9.05 (dd, ³J(H²,H³) = 5 Hz, ⁴J(H²,H⁴) = 1 Hz, ³J(H²,Pt) = 31 Hz, 1H; bzq-H²), 8.63 (dd, ⁴J(H⁴,H⁵) = 1 Hz, ³J(H⁴,H³) = 8 Hz, 1H; bzq-H⁴), 8.29 (d, ³J(H⁹,H⁸) = 7 Hz, ³J(H⁹,Pt) = 50 Hz, 1H; bzq-H⁹), 7.86 (AB, 1H; bzq-H⁵), 7.71 (AB, ³J(H⁶,H⁵) = 9 Hz, 1H; bzq-H⁶), 7.69 (m, 2H; bzq-H³, bzq-H⁷), 7.59 (dd, ³J(H⁸,H⁷) = ³J(H⁸,H⁹) = 7 Hz, 1H; bzq-H⁸), 1.76 ppm (s, 9H; CN*t*Bu-

CH₃); ¹H NMR (400.13 MHz, CD₂Cl₂, 25 °C, TMS): δ = 8.88 (dd, ³J(H²,H³) = 5 Hz, ⁴J(H²,H⁴) = 1 Hz, ³J(H²,Pt) = 31 Hz, 1H; bzq-H²), 8.42 (dd, ³J(H⁴,H⁵) = 8 Hz, 1H; bzq-H⁴), 8.27 (dd, ⁴J(H⁹,H⁷) = 1 Hz, ³J(H⁹,H⁸) = 7 Hz, ³J(H⁹,Pt) = 51 Hz, 1H; bzq-H⁹), 7.81 (AB, ³J(H⁵,H⁶) = 9 Hz, 1H; bzq-H⁵), 7.67 (dd, ³J(H⁷,H⁸) = 8 Hz, 1H; bzq-H⁷), 7.61 (dd, 1H; bzq-H⁸), 7.59 (AB, 1H; bzq-H⁶), 7.53 ppm (dd, 1H; bzq-H³); ¹³C{¹H} NMR (**1'**, 100.6 MHz, CD₂Cl₂, 25 °C, TMS): δ = 111.1 ppm (s, ¹J(C,Pt) = 1429 Hz; ¹³CN_{trans-N}); IR: ν̄ = 2209 (s, C≡N-*t*Bu), 2188 (s), 2123 cm⁻¹ (s, C≡N⁻); MS (ES⁺): *m/z* (%): 482.9 (100) [*M*⁺]; elemental analysis calcd (%) for C₁₉H₁₇N₃Pt: C 47.30, H 3.55, N 8.71; found: C 47.28, H 3.48, N 8.69.

Synthesis of (SP-4-3)-[Pt(bzq)(CN)(CN-Xyl)] (**2**)

Method a) KCN (0.017 g, 0.27 mmol) and MeOH (10 mL) were added to a solution of [Pt(bzq)(CN-Xyl)]ClO₄ (0.183 g, 0.25 mmol) in CH₂Cl₂ (8 mL), and the mixture was stirred. The initially yellow solution turned orange, and after 15 min a yellow solid precipitated. The solvent was evaporated to dryness, CH₂Cl₂ (65 mL) was added to the residue, and the suspension was filtered. The resulting solution was evaporated to ca. 2 mL to give a yellow solid **2** that was filtered and washed with Et₂O (5 mL). Yield: 0.120 g, 91%. **Method b)** AgClO₄ (0.062 g, 0.29 mmol) was added to a solution of [Pt(bzq)Cl(CN-Xyl)] (0.162 g, 0.30 mmol) in dichloromethane/acetone (25/2 mL) at 0 °C. The mixture was stirred for 1 h and it was then filtered through Celite. KCN (0.019 g, 0.29 mmol) and MeOH (2 mL) were added to the resulting solution; the mixture was stirred for one hour at 0 °C and then left to reach RT. It was then evaporated to dryness, the residue was treated with CH₂Cl₂ (10 mL), and the mixture was filtered through Celite. The evaporation of the solvent to 2 mL caused the precipitation of complex **2** as a yellow solid. Yield: 0.077, 48%. ¹H NMR (400.13 MHz, CD₂Cl₂, 25 °C, TMS): δ = 9.13 (d, ³J(H²,H³) = 5 Hz, ³J(H²,Pt) = 30 Hz, 1H; bzq-H²), 8.49 (d, ³J(H⁴,H³) = 8 Hz, 1H; bzq-H⁴), 8.36 (d, ³J(H⁹,H⁸) = 7 Hz, ³J(H⁹,Pt) = 51 Hz, 1H; bzq-H⁹), 7.87 (AB, ³J(H⁵,H⁶) = 9 Hz, 1H; bzq-H⁵), 7.71 (m, 2H; bzq-H⁷, bzq-H⁸), 7.65 (AB, 1H; bzq-H⁶), 7.59 (dd, 1H; bzq-H³), 7.39 (t, ³J(H³,H⁴,H⁵) = 8 Hz, 1H; CNXyl-H⁴), 7.26 (d, 2H; CNXyl-H³,H⁵) 2.64 ppm (s, 6H; CNXyl-CH₃); ¹³C{¹H} NMR (**2'**, 100.6 MHz, CD₂Cl₂, 25 °C, TMS): δ = 110.5 ppm (s, ¹J(C,Pt) = 1424 Hz; ¹³CN_{trans-N}); IR: ν̄ = 2172 (s, C≡N-Xyl), 2131 cm⁻¹ (s, C≡N⁻). MS (ES⁺): *m/z* (%): 531.0 (100) [*M*⁺]; elemental analysis calcd (%) for C₂₃H₁₇N₃Pt: C 52.07, H 3.40, N 7.65.

Synthesis of (SP-4-3)-[Pt(bzq)(CN)(CN-2-Np)] (**3**):

Method a) KCN (0.0158 g, 0.24 mmol) and MeOH (25 mL) were added to a solution of [Pt(bzq)(CN-2-Np)]ClO₄ (0.189 g, 0.24 mmol) in CH₂Cl₂ (35 mL) and the mixture was stirred. The initially yellow solution turned red, and after 50 min the solvent was evaporated to dryness. CH₂Cl₂ (200 mL) was added to the residue, and the suspension was filtered. Evaporation of the resulting solution to dryness gave a fuchsia solid **3** that was filtered and washed with Et₂O (30 mL). Yield: 0.114 g, 85%. **Method b)** AgClO₄ (0.082 g, 0.39 mmol) was added to a solution of [Pt(bzq)Cl(CN-2-Np)] (0.223 g, 0.39 mmol) in acetonitrile (30 mL) at room temperature, and the mixture was stirred for 15 min. The solution was filtered through Celite, and KCN (0.026 g, 0.39 mmol) and MeOH (4 mL) were added to the resulting solution. After one hour the solvent was evaporated to dryness and the residue was washed with water (2 × 10 mL). It was then treated with acetone (20 mL) and heated at refluxed for 45 min. The precipitated fuchsia solid **3** was filtered from the hot mixture. Yield: 0.145, 67%. ¹H NMR (400.13 MHz, CD₂Cl₂, 25 °C, TMS): δ = 9.07 (dd, ³J(H²,H³) = 5 Hz, ⁴J(H²,H⁴) = 1 Hz, ³J(H²,Pt) = 31 Hz, 1H; bzq-H²), 8.39 (dd, ³J(H⁴,H³) = 8 Hz, 1H; bzq-H⁴), 8.28 (dd, ⁴J(H⁹,H⁷) = 1 Hz, ³J(H⁹,H⁸) = 7 Hz, ³J(H⁹,Pt) = 51 Hz, 1H; bzq-H⁹), 8.21 (s, 1H; C₂Np-H¹), 7.75 ppm (m, 11H; bzq-H³, bzq-H⁵, bzq-H⁶, bzq-H⁷, bzq-H⁸, C₂Np-H³, C₂Np-H⁴, C₂Np-H⁵, C₂Np-H⁶, C₂Np-H⁷, C₂Np-H⁸). ¹³C{¹H} NMR (**3'**, 75.43 MHz, CD₂Cl₂, 25 °C, TMS): δ = 110.4 ppm (s, ¹J(C,Pt) = 1426 Hz; ¹³CN_{trans-N}); IR: ν̄ = 2181 (s, C≡N-2-Np), 2131 cm⁻¹ (s, C≡N⁻); MS (ES⁺): *m/z* (%): 553.0 (60) [*M*⁺]; elemental analysis calcd (%) for C₂₅H₁₅N₃Pt: C 54.35, H 2.74, N 7.61. Found: C 54.53, H 2.67, N 7.50.

Synthesis of (SP-4-2)-[Pt(bzq)(C≡CPh)(CN-Xyl)] (4)

HC≡CPh (31 μL, 0.28 mmol), CuI (6.5 mg, 0.03 mmol), and NEt₃ (1 mL) were added to a yellow solution of [Pt(bzq)Cl(CN-Xyl)] (0.100 g, 0.18 mmol) in deoxygenated CHCl₃ (15 mL) under Ar. After 1 h of stirring, the solvent was evaporated to dryness and the residue was treated with 2-propanol (15 mL), giving a yellow solid **4**. Yield: 0.098 g, 88%. ¹H NMR (400.13 MHz, CDCl₃, 25 °C, TMS): δ = 10.03 (d, ³J(H²,H³) = 5 Hz, ³J(H²,Pt) = 37 Hz, 1H; bzq-H²), 8.37 (d, ³J(H⁴,H³) = 8 Hz, 1H; bzq-H⁴), 8.06 (d, ³J(H⁹,H⁸) = 7 Hz, ³J(H⁹,Pt) = 39 Hz, 1H; bzq-H⁹), 7.82 (AB, ³J(H⁵,H⁶) = 9 Hz, 1H; bzq-H⁵), 7.68 (AB, 1H; bzq-H⁶), 7.58 (m, 3H; bzq-H³, bzq-H⁷, bzq-H⁸), 7.26 (m, 3H; CNXyl-H³,H⁴,H⁵), 2.66 ppm (s, 6H; CNXyl-CH₃). ¹³C{¹H} NMR (100.6 MHz, CDCl₃, 25 °C, TMS): δ = 159.1 (s, ¹J(C-Pt) = 712 Hz; bzq-C¹⁰), 158.1 (s, ²J(C-Pt) = 61 Hz, bzq-C¹²), 151.4 (s, ²J(C-Pt) = 41 Hz; bzq-C²), 148.0 (s, ¹J(C-Pt) = 23 Hz, 1C, bzq), 143.0 (s, ¹J(Pt-C) = 21, 1C, bzq), 138.6–121.5 (8C bzq and aromatics), 118.3 (s, ¹J(Pt-C) = 848, C_α≡C_β, C_α *trans* to C_{orthomet}), 107.8 (s, ²J(Pt-C) = 220, C_α≡C_β, C_β *trans* to C_{orthomet}), 19.0 ppm (s; Xyl-CH₃); IR: ν̄ = 2178 (s, C≡N-Xyl), 2167 (s), 2119 cm⁻¹ (s, C≡C); MS (MALDI-TOF+): *m/z* (%): 605.3 (50) [M⁺], 1210.6 (40) [2M]⁺, elemental analysis calcd (%) for C₃₀H₂₂N₂Pt: C 59.50, H 3.66, N 4.63. Found: C 58.97, H 3.84, N 4.47.

X-ray Structure Determination

Crystal data and other details of the structure analysis are presented in Table 4. Suitable crystals for X-ray diffraction studies were obtained by slow diffusion of *n*-hexane into concentrated solutions of the complexes in CHCl₃ at 4 °C (**1** and **2**) –30 °C (**4**). The crystals were mounted at the end of a quartz fiber. The radiation used was graphite monochromated MoK_α (λ = 0.71073 Å). For **1**-CHCl₃ and **2**-CHCl₃, X-ray intensity data were collected on an Oxford Diffraction Xcalibur CCD diffractometer,

Table 4. Crystal data and structure refinement for complexes **1**-CHCl₃, **2**-CHCl₃ and **4**.

	1 -CHCl ₃	2 -CHCl ₃	4
formula	C ₁₀ H ₁₇ N ₃ Pt-CHCl ₃	C ₂₃ H ₁₇ N ₃ Pt-CHCl ₃	C ₃₀ H ₂₂ N ₂ Pt
<i>M</i> _r [g mol ⁻¹]	601.81	649.85	605.59
<i>T</i> [K]	100(1)	100(1)	173(1)
λ [Å]	0.71073	0.71073	0.71073
crystal system	orthorhombic	triclinic	monoclinic
space group	<i>Pnma</i>	<i>P1̄</i>	<i>P2₁/c</i>
<i>a</i> [Å]	25.8987(6)	7.3178(2)	12.8868(13)
<i>b</i> [Å]	6.6532(1)	10.2903(3)	8.8689(9)
<i>c</i> [Å]	23.9980(6)	15.2916(5)	19.8272(16)
α [°]	90	93.787(2)	90
β [°]	90	95.044(3)	96.994(6)
γ [°]	90	103.757(2)	90
<i>V</i> [Å ³]	4135.05(16)	1109.62(6)	2249.2(4)
<i>Z</i>	8	2	4
ρ [g cm ⁻³]	1.933	1.945	1.788
μ [mm ⁻¹]	7.184	6.701	6.260
<i>F</i> (000)	2304	624	1176
2θ range [°]	8.4–57.7	7.8–54.2	5.0–51.4
no. of reflns collected	25140	12627	4241
no. of unique reflns	5383	4817	4241
<i>R</i> (int)	0.0259	0.0179	0.0000
final <i>R</i> indices			
[<i>I</i> > 2θ(<i>I</i>)] ^[a]			
<i>R</i> ₁	0.0329	0.0154	0.0659
<i>wR</i> ₂	0.0674	0.0411	0.1360
<i>R</i> indices (all data)			
<i>R</i> ₁	0.0432	0.0165	0.1309
<i>wR</i> ₂	0.0686	0.0413	0.1650
Goodness-of-fit on <i>F</i> ² [b]	1.281	1.063	1.064

[a] $R_1 = \sum(|F_o| - |F_c|) / \sum |F_o|$. $wR_2 = [\sum w(F_o^2 - F_c^2)^2 / \sum w(F_o^2)^2]^{1/2}$. [b] Goodness-of-fit = $[\sum w(F_o^2 - F_c^2)^2 / (n_{\text{obs}} - n_{\text{param}})]^{1/2}$.

and the diffraction frames were integrated and corrected for absorption using the Crysalis RED package.^[38] For **4**, X-ray intensity data were collected with a Nonius κ-CCD area-detector diffractometer using graphite-monochromated Mo K_α radiation. Images were processed using the DENZO and SCALEPACK suite of programs,^[39] and the absorption correction was performed using XABS2.^[40] The structures were solved by Patterson and Fourier methods and refined by full-matrix least squares on *F*² with SHELXL-97.^[41] All non-hydrogen atoms were assigned anisotropic displacement parameters and refined without positional constraints. All hydrogen atoms were constrained to idealized geometries and assigned isotropic displacement parameters equal to 1.2 times the *U*_{iso} values of their attached parent atoms (1.5 times for the methyl hydrogen atoms). Full-matrix least-squares refinement of these models against *F*² converged to final residual indices given in Table 4.

Acknowledgements

This work was supported by the Spanish MICINN [Projects CTQ2008-06669-C02-01,02 and the Gobierno de Aragón (Grupo Consolidado: Química Inorgánica y de los Compuestos Organometálicos). P.B. and A.D. acknowledge the support of a FPI grant from the MICINN.

- [1] B. M. Anderson, S. K. Hurst, *Eur. J. Inorg. Chem.* **2009**, 3041–3054.
- [2] M. Atoji, J. W. Richardson, R. E. Rundle, *J. Am. Chem. Soc.* **1957**, 79, 3017–3020.
- [3] a) J. R. Miller, *J. Chem. Soc.* **1961**, 4452–4457; b) J. Breimi, D. Brovelli, W. Caseri, G. Hähner, P. Smith, T. Tervoort, *Chem. Mater.* **1999**, 11, 977–994.
- [4] a) S. M. Drew, D. E. Janzen, K. R. Mann, *Anal. Chem.* **2002**, 74, 2547–2555; b) S. M. Drew, D. E. Janzen, C. E. Buss, D. I. MacEwan, K. M. Dublin, K. R. Mann, *J. Am. Chem. Soc.* **2001**, 123, 8414–8415.
- [5] S. M. Drew, J. E. Mann, B. J. Marquardt, K. R. Mann, *Sens. Actuators B* **2004**, 97, 307–312.
- [6] L. H. Doerrler, *Dalton Trans.* **2010**, 39, 3543–3553.
- [7] G. Gliemann, H. Yersin, *Structure and Bonding*, Springer, Berlin, **1985**.
- [8] T. J. Wadas, Q.-M. Wang, Y.-J. Kim, C. Flashenreim, T. M. Blanton, R. Eisenberg, *J. Am. Chem. Soc.* **2004**, 126, 16841–16849.
- [9] V. W. W. Yam, K. M. C. Wong, N. Zhu, *J. Am. Chem. Soc.* **2002**, 124, 6506–6507.
- [10] V. W. W. Yam, K. H. Y. Chan, K. M. C. Wong, N. Zhu, *Chem. Eur. J.* **2005**, 11, 4535–4543.
- [11] J. A. Bailey, M. G. Hill, R. E. Marsh, V. M. Miskowski, W. P. Schaefer, H. B. Gray, *Inorg. Chem.* **1995**, 34, 4591–4599.
- [12] a) R. J. Osborn, D. Rogers, *J. Chem. Soc. Dalton Trans.* **1974**, 1002–1004; b) W. B. Connick, L. M. Henling, R. E. Marsh, H. B. Gray, *Inorg. Chem.* **1996**, 35, 6261–6265.
- [13] a) W. B. Connick, L. M. Henling, R. E. Marsh, *Acta Crystallogr. Sect. B* **1996**, 52, 817–822; b) M. Kato, C. Kosuge, K. Morii, J. S. Ahn, H. Kitagawa, T. Mitani, M. Matsushita, T. Kato, S. Yano, M. Kimura, *Inorg. Chem.* **1999**, 38, 1638–1641.
- [14] W. B. Connick, R. E. Marsh, W. P. Schaefer, H. B. Gray, *Inorg. Chem.* **1997**, 36, 913–922.
- [15] C. E. Buss, K. R. Mann, *J. Am. Chem. Soc.* **2002**, 124, 1031–1039.
- [16] A. G. Dylla, D. E. Janzen, M. K. Pomije, K. R. Mann, *Organometallics* **2007**, 26, 6243–6247.
- [17] Y. Sun, K. Ye, H. Zhang, J. Zhang, L. Zhao, B. Li, G. Yang, B. Yang, Y. Wang, S. W. Lai, C. M. Che, *Angew. Chem.* **2006**, 118, 5738–5741; *Angew. Chem. Int. Ed.* **2006**, 45, 5610–5613.
- [18] A. Díez, J. Forniés, C. Larraz, E. Lalinde, J. A. López, A. Martín, M. T. Moreno, V. Sicilia, *Inorg. Chem.* **2010**, 49, 3239–3259.
- [19] a) I. Eryazici, C. N. Moorefield, G. R. Newkome, *Chem. Rev.* **2008**, 108, 1834–1895; b) J. Moussa, K. M. C. Wong, L. M. Chamoreau, H. Amouri, V. W. W. Yam, *Dalton Trans.* **2007**, 3526–3530.
- [20] S. Y. L. Leung, A. Y. Y. Tam, C. H. Tao, H. S. Chow, V. W. W. Yam, *J. Am. Chem. Soc.* **2012**, 134, 1047–1056.

- [21] C. Janiak, *J. Chem. Soc. Dalton Trans.* **2000**, 3885–3896.
- [22] M. Kato, *Bull. Chem. Soc. Jpn.* **2007**, *80*, 287–294.
- [23] C. Po, A. Y. Y. Tam, K. M. C. Wong, V. W. W. Yam, *J. Am. Chem. Soc.* **2011**, *133*, 12136–12143.
- [24] a) J. Ni, X. Zhang, Y. H. Wu, L. Y. Zhang, Z. N. Chen, *Chem. Eur. J.* **2011**, *17*, 1171–1183; b) X. Zhang, J. Y. Wang, J. Ni, L. Y. Zhang, Z. N. Chen, *Inorg. Chem.* **2012**, *51*, 5569–5579; c) X. Zhang, B. Li, Z. H. Chen, Z. N. Chen, *J. Mater. Chem.* **2012**, *22*, 11427–11441.
- [25] a) C. L. Exstrom, J. R. Sowa, Jr., C. A. Daws, D. Janzen, K. R. Mann, G. A. Moore, F. F. Stewart, *Chem. Mater.* **1995**, *7*, 15–17; b) C. A. Daws, C. L. Exstrom, J. R. Sowa Jr., K. R. Mann, *Chem. Mater.* **1997**, *9*, 363–368; c) Y. Kunugi, L. L. Miller, K. R. Mann, M. K. Pomije, *Chem. Mater.* **1998**, *10*, 1487–1489; d) J. W. Grate, L. K. Moore, D. E. Janzen, D. J. Veltkamp, S. Kaganove, S. M. Drew, K. R. Mann, *Chem. Mater.* **2002**, *14*, 1058–1066; e) C. E. Buss, C. E. Anderson, M. K. Pomije, C. M. Lutz, D. Britton, K. R. Mann, *J. Am. Chem. Soc.* **1998**, *120*, 7783–7790.
- [26] S. M. Drew, L. I. Smith, K. A. McGee, K. R. Mann, *Chem. Mater.* **2009**, *21*, 3117–3124.
- [27] G. Aullón, S. Alvarez, *Chem. Eur. J.* **1997**, *3*, 655–664.
- [28] J. P. H. Charmant, J. Forniés, J. Gómez, E. Lalinde, R. I. Merino, M. T. Moreno, G. Orpen, *Organometallics* **1999**, *18*, 3353–3358.
- [29] J. Forniés, S. Fuertes, C. Larráz, A. Martín, V. Sicilia, A. C. Tshipis, *Organometallics* **2012**, *31*, 2729–2740.
- [30] S. Fernández, J. Forniés, B. Gil, J. Gómez, E. Lalinde, *Dalton Trans.* **2003**, 822–830.
- [31] a) A. Díez, J. Forniés, S. Fuertes, E. Lalinde, C. Larráz, J. A. López, A. Martín, M. T. Moreno, V. Sicilia, *Organometallics* **2009**, *28*, 1705; b) A. Díez, J. Forniés, A. García, E. Lalinde, M. T. Moreno, *Inorg. Chem.* **2005**, *44*, 2443–2453; c) J. Forniés, S. Fuertes, A. Martín, V. Sicilia, B. Gil, E. Lalinde, *Dalton Trans.* **2009**, 2224–2234.
- [32] a) B.-H. Xia, C. M. Che, D. L. Phillips, K.-H. Leung, K. K. Cheung, *Inorg. Chem.* **2002**, *41*, 3866–3875; b) M.-L. Flay, H. Vahrenkamp, *Eur. J. Inorg. Chem.* **2003**, 1719–1726; c) J. Forniés, J. Gómez, E. Lalinde, M. T. Moreno, *Chem. Eur. J.* **2004**, *10*, 888–898.
- [33] a) S. W. Lai, H. W. Lam, W. Lu, K. K. Cheung, C. M. Che, *Organometallics* **2002**, *21*, 226–234; b) J. Vicente, A. Arcas, J. M. Fernández-Hernández, G. Aullón, D. Bautista, *Organometallics* **2007**, *26*, 6155–6169; c) P. J. Martellaro, S. K. Hurst, R. Larson, E. H. Abbott, E. S. Peterson, *Inorg. Chim. Acta* **2005**, *358*, 3377–3383.
- [34] J. Forniés, S. Fuertes, J. A. López, A. Martín, V. Sicilia, *Inorg. Chem.* **2008**, *47*, 7166–7176.
- [35] a) P. H. Lanoë, H. Le Bozec, J. A. G. Williams, J. L. Fillaut, V. Guerschais, *Dalton Trans.* **2010**, 39, 707–710; b) R. Liu, Y. Li, H. Zhu, W. Sun, *J. Phys. Chem. A* **2010**, *114*, 12639–12645; c) W. Lu, B. X. Mi, M. C. W. Chan, Z. Hui, C. M. Che, N. Zhu, S. T. Lee, *J. Am. Chem. Soc.* **2004**, *126*, 4958–4971.
- [36] a) V. W. W. Yam, K. H. Y. Chan, K. M. C. Wong, B. W. K. Chu, *Angew. Chem.* **2006**, *118*, 6315; *Angew. Chem. Int. Ed.* **2006**, *45*, 6169; b) C. K. Koo, K. L. Wong, K. C. Lau, W. Y. Wong, M. H. W. Lam, *Chem. Eur. J.* **2009**, *15*, 7689–7697; c) K. M. C. Wong, V. W. W. Yam, *Acc. Chem. Res.* **2011**, *44*, 424–434; d) V. Sicilia, J. Forniés, J. M. Casas, A. Martín, J. A. López, C. Larráz, P. Borja, C. Ovejero, D. Tordera, H. Bolink, *Inorg. Chem.* **2012**, *51*, 3427–3435.
- [37] a) C. T. Liao, H. H. Chen, H. F. Hsu, A. Pollock, H. H. Yeh, Y. Chi, K. W. Wang, C. H. Lai, G. H. Lee, C. W. Shih, P. T. Chou, *Chem. Eur. J.* **2011**, *17*, 546–556; b) X. Zhou, H. X. Zhang, Q. J. Pan, M. X. Li, Y. Wang, C. M. Che, *Eur. J. Inorg. Chem.* **2007**, 2181–2188.
- [38] *CrysAlis RED Program for X-ray CCD camera data reduction*, Oxford Diffraction Ltd, Oxford, UK, **2005–2006**.
- [39] Z. Otwinowski, W. Minor in *Methods in Enzymology*, Vol. 276A (Eds.: C. V. Carter, Jr., R. M. Sweet), Academic Press, New York, **1997**, p. 307.
- [40] S. Parkin, B. Moezzi, H. Hope, *J. Appl. Crystallogr.* **1995**, *28*, 53–56.
- [41] G. M. Sheldrick, *SHELXL-97 Program for Crystal Structure Determination*, University of Göttingen, Göttingen, Germany, **1997**.

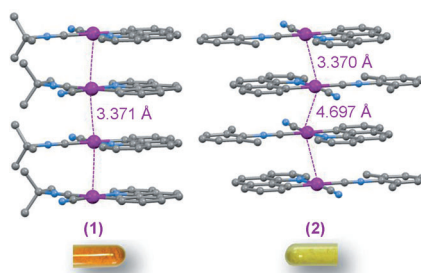
Received: June 29, 2012
Published online: ■ ■ ■, 0000

FULL PAPER

Platinum Complexes

Juan Forniés,* Violeta Sicilia,*
Pilar Borja, José M. Casas,
Alvaro Díez, Elena Lalinde,
Carmen Larraz, Antonio Martín,
M. Teresa Moreno ———— ■■■■—■■■■

 **Luminescent Benzoquinolate-Isocyanide Platinum(II) Complexes: Effect of Pt...Pt and π ... π Interactions on their Photophysical Properties**



Shining bright: New benzoquinolate isocyanide platinum(II) complexes, including the bright luminescent compounds (SP-4-3)-[Pt(bzq)(CN)(CNR)] (R = *t*Bu (**1**), Xyl(**2**)), have been isolated as pure isomers. The title weak intermolecular interactions are responsible for their photophysical properties.